

## Geophysical Research Letters®

## RESEARCH LETTER

10.1029/2022GL101814

## Key Points:

- The climatological impacts of tropical cyclone (TC) winds on El Niño-Southern Oscillation (ENSO) are investigated for the first time in a fully coupled Earth system model
- TC winds impact ENSO magnitude, frequency, and the occurrence of strong to extreme El Niño events
- Model proved that TC winds affect El Niño by enhancing the thermocline feedback and the zonal advection feedback

## Supporting Information:

Supporting Information may be found in the online version of this article.

## Correspondence to:

H. Li,  
huili7@ucar.edu

## Citation:

Li, H., Hu, A., & Meehl, G. A. (2023). Role of tropical cyclones in determining ENSO characteristics. *Geophysical Research Letters*, 50, e2022GL101814. <https://doi.org/10.1029/2022GL101814>

Received 21 OCT 2022

Accepted 15 FEB 2023

## Author Contributions:

**Conceptualization:** Hui Li, Aixue Hu, Gerald A. Meehl  
**Data curation:** Hui Li  
**Formal analysis:** Hui Li  
**Funding acquisition:** Gerald A. Meehl  
**Investigation:** Hui Li  
**Methodology:** Hui Li, Aixue Hu, Gerald A. Meehl  
**Project Administration:** Gerald A. Meehl  
**Software:** Hui Li  
**Supervision:** Aixue Hu, Gerald A. Meehl  
**Validation:** Hui Li, Aixue Hu  
**Visualization:** Hui Li  
**Writing – original draft:** Hui Li

© 2023. The Authors.

This is an open access article under the terms of the [Creative Commons Attribution-NonCommercial-NoDerivs License](#), which permits use and distribution in any medium, provided the original work is properly cited, the use is non-commercial and no modifications or adaptations are made.

## Role of Tropical Cyclones in Determining ENSO Characteristics

Hui Li<sup>1</sup> , Aixue Hu<sup>1</sup> , and Gerald A. Meehl<sup>1</sup> 

<sup>1</sup>Climate and Global Dynamics Laboratory, National Center for Atmospheric Research, Boulder, CO, USA

**Abstract** El Niño-Southern Oscillation (ENSO) can effectively modulate global tropical cyclone (TC) activity, but the role TCs may play in determining ENSO characteristics remains unclear. Here we investigate the impact of TC winds on ENSO using a suite of Earth system model experiments where we insert TC winds, extracted from a TC-permitting high-resolution simulation, into a low-resolution model configuration with nearly no intrinsic TCs. The presence of TC winds in the model increases ENSO power and shifts ENSO frequency closer to what we observe. TCs lead to an increase of strong to extreme El Niño events seen in observations and not simulated in the low-resolution model without intrinsic TCs, mainly through enhanced zonal advection feedback and thermocline feedback. Our results indicate that TCs play a fundamental role in producing the ENSO characteristics we experience today in the climate system and point to a two-way climatological interaction between TCs and ENSO.

**Plain Language Summary** El Niño-Southern Oscillation (ENSO) can influence global tropical cyclone (TC) activity by altering the large-scale conditions. TCs, as transient yet powerful weather events, can cause strong air-sea interactions over the tropical ocean that may consequently influence the climate mean state. Here we show how TCs could be essential to the characteristics of ENSO using a suite of Earth system model experiments where we insert TC winds, extracted from a high-resolution model simulation, into a low-resolution model simulation with nearly no intrinsic TCs. The added TC winds in the model increases ENSO power and shifts ENSO frequency closer to the observations. TCs lead to an increase of strong to extreme El Niño events seen in observations and not simulated in the low-resolution model without intrinsic TCs. Our results indicate that TCs play a fundamental role in producing the ENSO characteristics we experience today in the climate system and point to a previously unidentified two-way climatological interaction between TCs and ENSO.

## 1. Introduction

El Niño-Southern Oscillation (ENSO) is the primary source for interannual variability over the tropical Pacific, with wide-ranging impacts on the global climate (Clarke, 2008; Philander, 1990; Sarachik & Cane, 2010). It is well accepted that ENSO can effectively modulate global tropical cyclone (TC) activity by altering the large-scale atmospheric and oceanic conditions (Camargo et al., 2010; Chan, 2000; Chand et al., 2013; Lander, 1994; Sobel et al., 2016; B. Wang & Chan, 2002; see Lin et al., 2020 for a review). For example, El Niño years tend to suppress TC activity in the North Atlantic and shift the TC genesis in the North Pacific toward the international date line, while La Nina years have the opposite effect (Bell et al., 2014; Camargo et al., 2007).

ENSO is typically framed as a neutrally stable natural mode of oscillation resulting from tropical ocean-atmosphere interactions, sustained and diversified by stochastic atmospheric forcing (Fedorov & Philander, 2000, 2001; Kessler, 2002; Philander & Fedorov, 2003; Thompson & Battisti, 2001). It has been argued that ENSO characteristics depend on the initial ocean state, the timing and strength of westerly wind bursts (WWBs), and the subsequent ocean-atmosphere interactions involving Kelvin wave propagation and warm pool expansion related to discharge and recharge of ocean heat content (Fedorov et al., 2015; Gebbie et al., 2007; Jin, 1997; Lengaigne et al., 2004; Lopez et al., 2013). All these critical factors are closely associated with TCs: TCs can contribute to a recharge of heat in the equatorial Pacific Ocean by increasing the upper ocean heat content via vertical mixing and downwelling motion (Emanuel, 2001; Fedorov et al., 2010; Li & Srivier, 2016, 2018; Li et al., 2022). Additionally, TCs are associated with the majority of WWBs over the equatorial Pacific that can affect ENSO (Harrison & Giese, 1991; Hartten, 1996; Keen, 1982; Lian et al., 2018; Liang & Fedorov, 2021).

Writing – review & editing: Aixue Hu,  
Gerald A. Meehl

The possibility of TCs' contribution to ENSO was first suggested by Sobel and Camargo (2005) and Camargo and Sobel (2005). Sobel and Camargo (2005) came up with the hypothesis that, in an El Niño year, stronger and longer-lived TCs that occur in the western tropical Pacific before the El Niño peak can enhance surface westerly anomalies there and subsequently increase the SST in the central and eastern equatorial Pacific, which helps to strengthen the incipient El Niño. Camargo and Sobel (2005) found significant correlations when the TC accumulated cyclone energy leads the Niño indices up to 6 months, pointing to TCs' contribution to a developing El Niño. Lian et al. (2019) used an intermediate coupled model with prescribed synthetic TC winds and found that TCs can add to the irregularity of ENSO and largely determine the magnitude and even the final state of the ENSO events. Q. Y. Wang et al. (2019) systematically studied the important role of western North Pacific TC activity in ENSO intensity on interannual timescales using observations and an intermediate-complexity model. They revealed two pathways that TCs affect ENSO on interannual timescales, by weakening the Walker Circulation and reducing the equatorial Pacific zonal thermocline gradient. They also found that feedback of the western North Pacific TCs can affect El Niño diversity (Q. Wang & Li, 2022).

Yet, no study to date has examined how the climatological presence of TCs in fully coupled Earth system models can be essential to producing ENSO characteristics. Understanding this TCs' contribution to ENSO is of great importance to how we view climatological processes and multi-scale interactions in the climate system. It is particularly relevant to today's generation of high-resolution climate modeling at TC-permitting resolution (i.e., finer than 25 km atmosphere grid spacing) where TCs are spontaneously simulated, and their impacts are inherently embedded within the modeled climate. The models' self-generated TCs may leave their marks on the simulated climate mean state, variability, and change under future warming (Li & Srivier, 2016, 2018; Li et al., 2022).

Given these potentially prominent roles of TCs in the climate system, here we aim to explore the impact of TC winds on the characteristics of ENSO and investigate the dynamical mechanisms in the context of a coupled Earth system model. Using the Community Earth System Model version 1.3 (CESM1.3), we design an experiment where we isolate TCs' impact by introducing realistic transient TC wind forcing extracted from a TC-permitting high-resolution atmospheric model at 0.25° horizontal resolution into a fully coupled lower resolution climate model at 1° resolution ("LR-TC") that does not inherently have TC strength winds ("LR-ctrl"), and these results are compared to two high-resolution coupled simulations with intrinsic TCs ("HR"—0.25° atmosphere coupled to 1° ocean, and "HR\_0.1"—0.25° atmosphere coupled to 0.1° ocean) (see Section 2). In a companion study (Li et al., 2022), we found that the added TC winds can have a broad impact on the large-scale climate. Particularly, the TC winds increase the equatorial upper ocean heat content, causing a warm temperature anomaly in the eastern equatorial Pacific, conducive to an El Niño-like SST pattern (Figures S1 and S3 in Supporting Information S1).

## 2. Model and Data

The model configuration and experiment design are described in detail in Li et al. (2022) and Text S1 in Supporting Information S1. Here we emphasize the most relevant aspects. We use two configurations the fully coupled CESM1.3 (Meehl et al., 2019) that differ in horizontal resolution. The first is a high-resolution configuration with a 0.25° "TC-permitting" atmosphere and 1° ocean (named "HR"), capable of simulating a realistic TC climatology and near-surface TC wind structure, that is used to provide TC wind forcing. The second is a low-resolution configuration with a nominal 1° atmosphere and 1° ocean ("LR") that is used for the main experiments. LR on average simulates around 11.4 TC-like storms globally per year, with no storm beyond Category 2 intensity, and with negligible impact on the ocean surface (Figure S2 in Supporting Information S1). We therefore regard the LR as a control climate (named "LR-ctrl") without strong TC winds' impact.

We extract surface TC winds from HR and prescribe the corresponding TC wind stress into the LR (named "LR-TC"). We use the TempestExtremes tracking algorithm (Ullrich & Zarzycki, 2017; Ullrich et al., 2021) for TC detection and tracking in HR. The tracked TC statistics are in general agreement with the observations, with an average of 88 global TCs annually, comparable to the observed 95 (Figure S1 in Supporting Information S1). Details of the TC statistics are described in Supporting Information S1 (Text S2).

For each detected TC day in HR, we take a 20° × 20° snapshot of the surface winds surrounding the TC center and calculate the corresponding surface wind stress offline. We then prescribe the TC wind stress into LR-TC as the model integrates. The prescribed TC wind stress preserves the timings and locations of each TC exactly as in the HR. LR-TC is the same as LR-ctrl except for the added TC wind stress, their differences therefore would

reveal the impact of TC winds on the simulated climate. All simulations are run with the preindustrial climate conditions for 100 years.

The simulated ENSO statistics are compared with the observation-based NOAA Extended Reconstructed Sea Surface Temperature (SST) V5 (ERSSTv5) reanalysis (Huang & Thorne, 2017) for the period of 1920–2018, as well as with another CESM1.3 high-resolution preindustrial simulation with 0.25° atmosphere and 0.1° eddy-resolving ocean (“HR\_0.1”) (Chang et al., 2020).

### 3. Results

#### 3.1. ENSO Statistics

Figures 1a and 1b show the time series of the monthly Niño 3.4 index in the LR-ctrl and LR-TC during the 100-year simulation. The LR-TC exhibits a stronger variability in the Niño 3.4 index and has more extreme ENSO events. The variability of the Niño 4 index also increases, but the changes are smaller than that of Niño 3.4 (Figure S4 in Supporting Information S1). The two models both feature ENSO phase-locking with the variance peaking toward the end of the calendar year (Figure 1c) (e.g., Ham & Kug, 2014; Harrison & Vecchi, 1999; Tziperman et al., 1997, 1998), though the timing of the peak in the models lags that in the observations by 1 month (December vs. the following January). Note that LR-TC has larger variance, and the seasonal cycle is more in line with the observations. It is possible that the added TC winds can affect the timing and strength of the coupled instability, and subsequently its seasonally varying amplification of Rossby and Kelvin ocean waves that are important for ENSO phase-locking (An & Wang, 2001; Tziperman et al., 1998).

The power spectrum of the Niño 3.4 index (Figure 1d) shows that the ENSO cycle in the observations and the model simulations spans a similar range of 2–7 years. The observed ENSO signal during 1920–2018 peaks at about 5 years, with a secondary peak at ~4 years. In comparison, the LR-ctrl shows a primary peak at 4 years, and the HR (with intrinsic TCs) shows a peak closer to 5 years. Meanwhile, the ENSO frequency in HR\_0.1 (0.25° atmosphere and 0.1° eddy-resolving ocean) is comparable to the observed with a slight shift toward a lower frequency. This suggests that the LR-ctrl without TCs is biased toward a higher ENSO frequency, the HR with intrinsic TCs can shift the ENSO frequency toward the observed, and the HR\_0.1 with eddy resolving ocean model makes the ENSO frequency even closer to the observed. On the other hand, with the added TC winds, the shape of the power spectrum in the LR-TC becomes more like the observations—with a primary peak at 5 years and a secondary peak at 4 years. This indicates that TC winds can enhance ENSO power and mitigate the model bias in ENSO frequency. Therefore, we could conclude that both atmosphere and ocean resolution can influence the simulated ENSO frequency and power, and TCs play a critical role in determining the ENSO frequency.

TCs' influence on ENSO frequency is likely due to the changes of the background mean state, particularly the upper ocean thermal structure in the tropical Pacific. LR-TC shows a reduced upper ocean zonal thermal gradient and a relaxed trade wind intensity (Figure S3 in Supporting Information S1), which likely contribute to the shift toward a lower ENSO frequency (An et al., 2008; Deng et al., 2010; Fedorov & Philander, 2000, 2001).

An increase of El Niño extremes is found in the LR-TC. During the 100-year simulation, the LR-ctrl has 23 El Niño events (defined as when Niño 3.4  $\geq 0.5^{\circ}\text{C}$ ), including 5 strong events (Niño 3.4  $\geq 1.5^{\circ}\text{C}$ ) and 2 extreme events (Niño 3.4  $\geq 2^{\circ}\text{C}$ ). The LR-TC also has 23 El Niño events, with 4 strong events and, remarkably, 6 extreme events—which is more consistent with the observations. The extreme El Niño in LR-TC are manifested as exceptionally warm equatorial SST anomalies (referenced to the long-term-mean monthly climatology in the respective simulations, averaged over 2°S–2°N for each El Niño from December to the following February) that span across the central to eastern equatorial Pacific, as shown in Figure 1e. In comparison, TCs' impact on La Niña is relatively small in the simulations (Figure S5 in Supporting Information S1). We therefore focus the analysis on El Niño in the following sections.

#### 3.2. Impact of TC Winds on El Niño Characteristics

How does the modeled El Niño in LR-TC relate to the added TC forcing? We first examine the relationship between the strong El Niño events and the near-equatorial TCs, which are considered as TC days occurring within 12°N–12°S over the western-to-central Pacific (120°E–200°E). The modeled 6-hourly TC occurrences within this region account for 5% of the global total, which is comparable with the observed 6%. Using a similar method

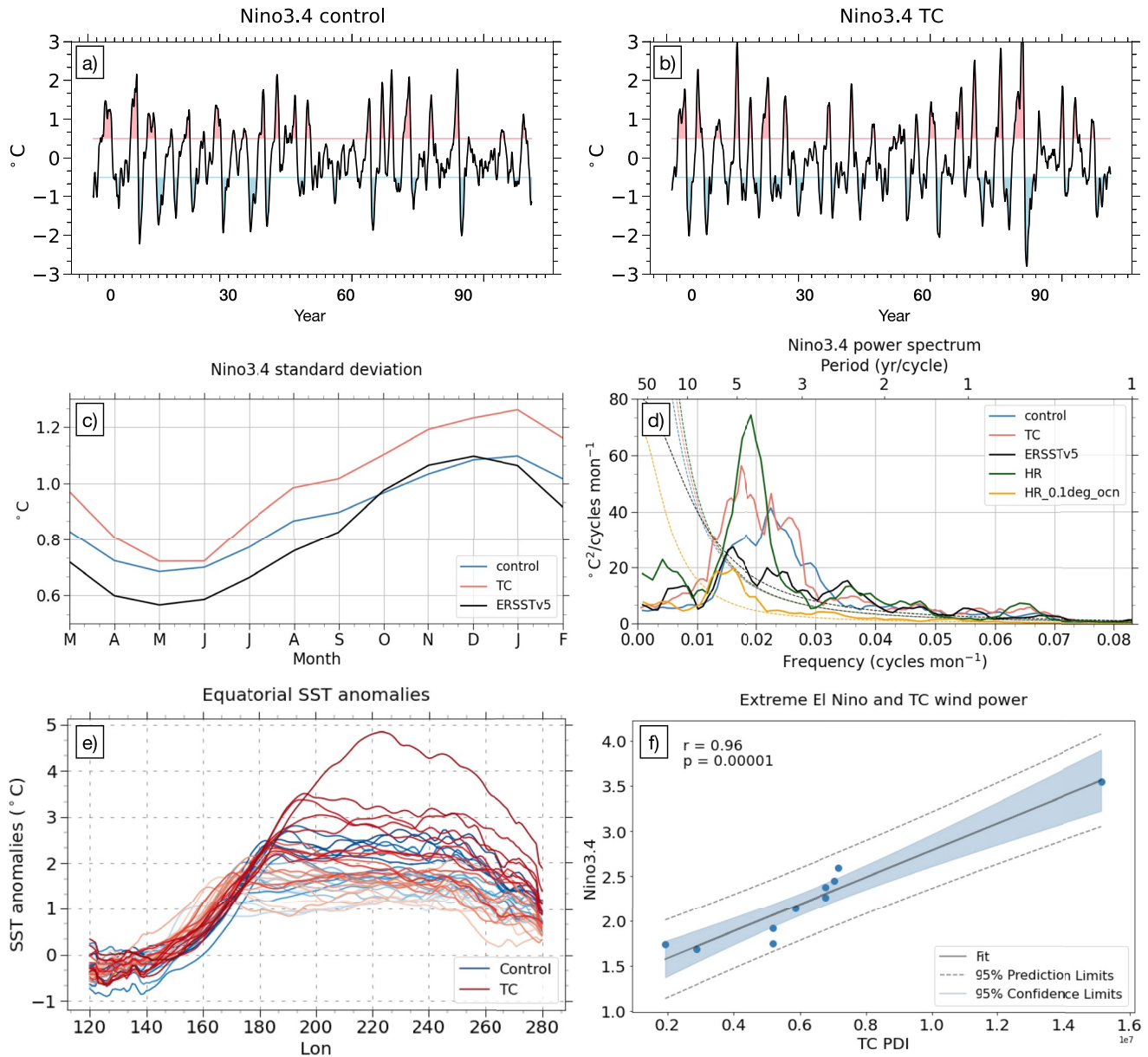


**Figure 1.** (a), (b) Niño3.4 time series in (a) the LR-ctrl and (b) the LR-TC. (c) Monthly standard deviation of the Niño3.4 time series in the ERSSTv5 reanalysis for the period of 1920–2018 (black), in the 100-year LR-ctrl (blue) and the LR-TC (red). (d) Power spectrum of the Niño3.4 index in the ERSSTv5 reanalysis (black) for the period of 1920–2018, in the 100-year LR-ctrl (blue), the LR-TC (red), the HR (green), and the HR\_0.1 with eddy resolving ocean (orange). Note that the ENSO frequency in the ERSSTv5 and the LR-TC peaks at ~5 year/cycle, while the control run peaks at 4 year/cycle. The comparisons reveal the impact of model resolution and TCs on ENSO frequency. (e) SST anomalies along the equatorial Pacific (averaged over 2°S–2°N) for each El Niño event in the LR-ctrl (blue) and the LR-TC (red). The SST anomalies are averaged over December to the following February. The color saturation, from light to dark, are sorted by the magnitude of the Niño3.4 index. (f) Scatterplot of the Niño3.4 index of strong El Niño events (Niño3.4 index  $\geq 1.5$ ) against the TC power dissipation index (TC PDI) integrated from May to December over the west equatorial Pacific (12°S–12°N, 120°E–200°E). PDI is scaled by  $2.1 \times 10^{-4}$ . The solid black line indicates the regression fit; The blue shading represents the 95% confidence interval of the regression, and the dashed black lines indicate 95% prediction interval. The Pearson correlation coefficient ( $r$ ), and the  $p$ -value ( $p$ ) of the regression are denoted in the figure.

as in Lian et al. (2019), we find that 45% of these TC days are associated with increased westerly wind anomalies (defined as westerly anomalies stronger than 3 m/s and within 2° longitudinal distance from the TC center) and can potentially affect El Niño. TC wind forcing is quantified using the TC power dissipation index (PDI), defined as  $\int_0^{\tau} V_{\max}^3 dt$ , where  $V_{\max}$  is the maximum surface wind speed at a given time of a storm, and  $\tau$  is the lifetime



of the TC event (Emanuel, 2005). The annual mean PDI within the near-equatorial western Pacific is generally consistent between the model ( $9.39 \times 10^{10} \text{ m}^3\text{s}^{-2}$ ) and the observations ( $9.55 \times 10^{10} \text{ m}^3\text{s}^{-2}$ ).

Figure 1f shows the scatter plot of the strength of each strong El Niño event against the integrated PDI of the near-equatorial western Pacific TCs. The TC PDI is integrated from May to December during each El Niño developing year. A strong positive correlation is identified with a correlation coefficient of 0.96. Note that the strongest event with an exceptionally high Niño index of  $3.8^\circ\text{C}$  also corresponds to the highest TC wind power. Removing the strongest event still yields a significant correlation of 0.87 (Figure S6 in Supporting Information S1). Since the added TCs in LR-TC do not depend on or respond to the modeled El Niño, this strong correlation indicates that TCs can significantly affect the strength of El Niño events. However, this significant correlation is valid only for the strong El Niño events—no discernable linear relationship is found between TCs and the weak to moderate events (correlation coefficient of 0.29). This suggests that TCs act to reinforce the strength of a developing El Niño provided sufficiently favorable conditions, such as a recharged ocean initial state and an extended warm pool edge (Figure S6 in Supporting Information S1), while their impact on weak El Niño events is limited.

TCs' impact on El Niño is further diagnosed via composite analysis of the evolution of SST, thermocline depth, and surface zonal current anomalies (Figure 2). The composite near-equatorial TC PDI (within  $12^\circ\text{S}$ – $12^\circ\text{N}$ ) are overlaid on top of the model differences (Figures 2c, 2f, and 2i). Compared to the LR-ctrl, the LR-TC has warmer SST during the El Niño peak season (November–February) across the central to eastern Pacific ( $150^\circ\text{E}$ – $90^\circ\text{W}$ ), indicative of a higher average El Niño strength. Note that LR-TC continues to be warmer than the LR-ctrl over the eastern equatorial Pacific at the end of the El Niño cycle, which occurs concomitantly with TC wind forcing during the following TC season.

The enhanced El Niño SST is consistent with the deeper thermocline anomalies that originate from the western Pacific and propagate eastward as the El Niño develops. The thermocline deepening is closely associated with the added TC winds (Figure 2f). To demonstrate the processes leading to the deepening of the thermocline, we conduct two case studies of the LR-TC, where we analyze the daily SST and thermocline depth anomalies and examine their connection to the near-equatorial TCs (Figure 3). The thermocline depth anomalies are filtered by a 20–100-day band pass to highlight the oceanic waves (Roundy & Kiladis, 2006). It is found that the early season TC winds over the western Pacific, acting as WWBs, can excite eastward-propagating downwelling Kelvin waves, leading to deeper equatorial thermocline and subsequent warming in the eastern equatorial Pacific. Meanwhile, the TC winds in the central to eastern Pacific can also excite westward upwelling Rossby waves. Such dynamics are similar to that found in the studies using intermediate-complexity coupled models in Lian et al. (2019), Q. Y. Wang et al. (2019), and Q. Wang and Li (2022). In addition, TC winds also cause strong surface wind stress (Figure S7 in Supporting Information S1) and eastward surface ocean currents (Figure 2i), critical for El Niño growth.

### 3.3. Impact of TC Winds on El Niño Dynamics

TCs' impact on El Niño dynamics is further investigated using a heat budget analysis of the ocean mixed layer temperature. Similar to Kug et al. (2009) and Kang et al. (2001), the temperature tendency is derived as:

$$\frac{\partial T'}{\partial t} = -u' \frac{\partial \bar{T}}{\partial x} - v' \frac{\partial \bar{T}}{\partial y} - w' \frac{\partial \bar{T}}{\partial z} - \bar{u} \frac{\partial T'}{\partial x} - \bar{v} \frac{\partial T'}{\partial y} - \bar{w} \frac{\partial T'}{\partial z} - u' \frac{\partial T'}{\partial x} - v' \frac{\partial T'}{\partial y} - w' \frac{\partial T'}{\partial z} + R,$$

where  $T$  is the average temperature in the upper 50 m,  $u$ , and  $v$  indicate zonal and meridional current,  $w$  is the vertical velocity at the bottom of the mixed layer. Overbars and primes indicate monthly climatology and anomalies, respectively.  $R$  is the residual term. All the variables are averaged over the equatorial band of  $2^\circ\text{S}$ – $2^\circ\text{N}$ . We focus on the thermocline feedback term ( $-\bar{w} \frac{\partial T'}{\partial z}$ ) and the zonal advection feedback term ( $-u' \frac{\partial \bar{T}}{\partial x}$ ), which are two major contributors to El Niño development (Jin et al., 2006; Ren & Jin, 2013), and are closely related to the TC-induced anomalies in thermocline depth and zonal current (Figure 2).

Figures 4a–4c show the composite Hovmöller diagrams of the thermocline feedback in both models and their differences. Both models show enhanced thermocline feedback over the eastern equatorial Pacific during El Niño development. Compared to LR-ctrl, the thermocline feedback in the LR-TC is increased by  $\sim 20\%$  during the El Niño peak season. The stronger thermocline feedback in the LR-TC generally co-occurs with enhanced TC wind power and closely follows the thermocline depth anomalies (Figure 2f), which confirms the impact of

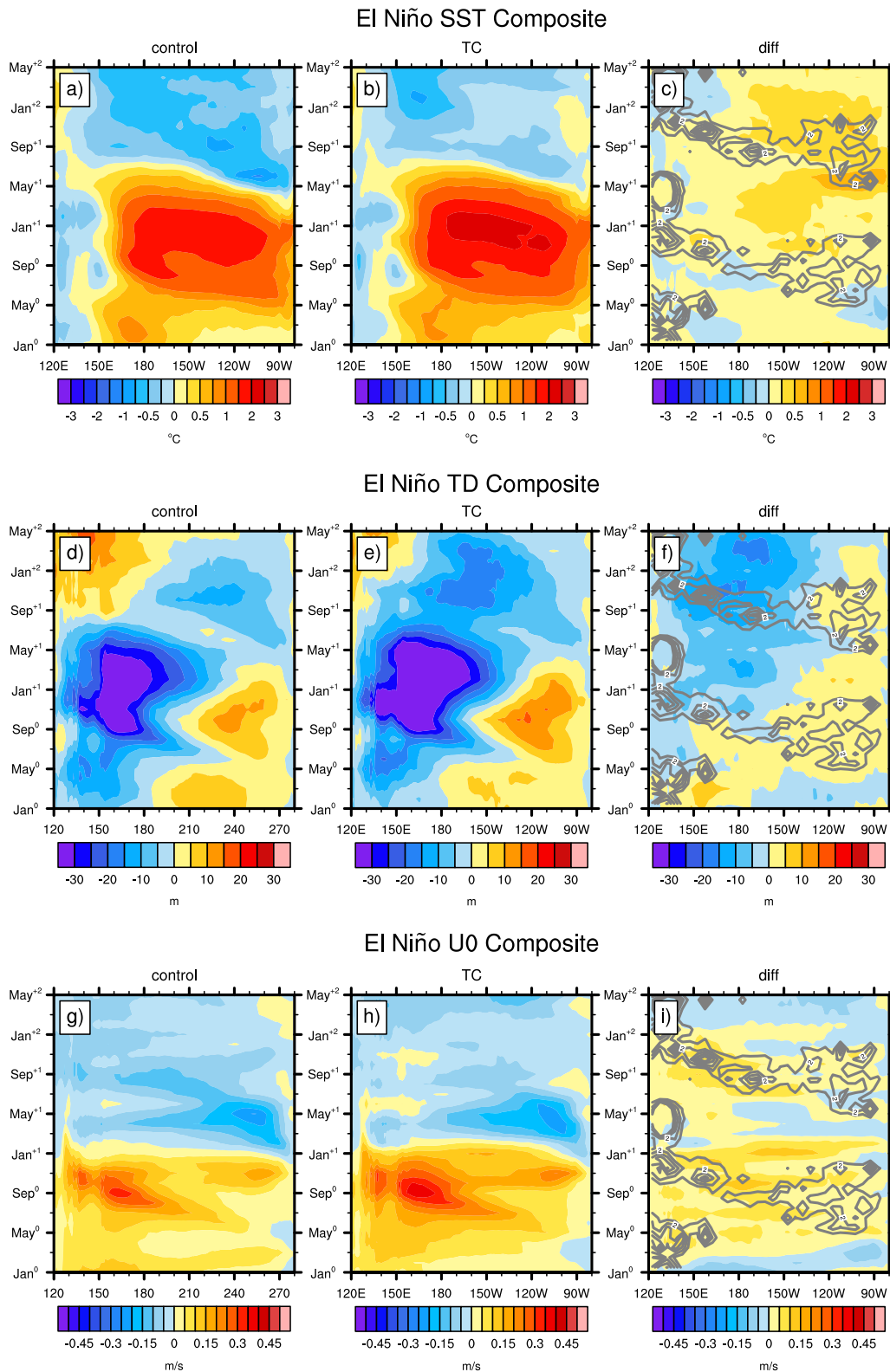


**Figure 2.** Composite Hovmöller diagrams of the equatorial Pacific (averaged over 2°S–2°N) (a)–(c) SST, (d)–(f) thermocline depth (defined as the depth of the largest temperature gradient) and (g)–(i) surface zonal current anomalies during El Niño events in the (a, d, g) LR-ctrl, (b, e, h) the LR-TC, and (c, f, i) their differences. The anomalies are calculated using the detrended data and are referenced to the long-term mean monthly climatology in the respective simulations. The gray contours in the right most columns represent the monthly integrated near-equatorial TC wind power (PDI, scaled by  $2.1 \times 10^{-8}$ ).

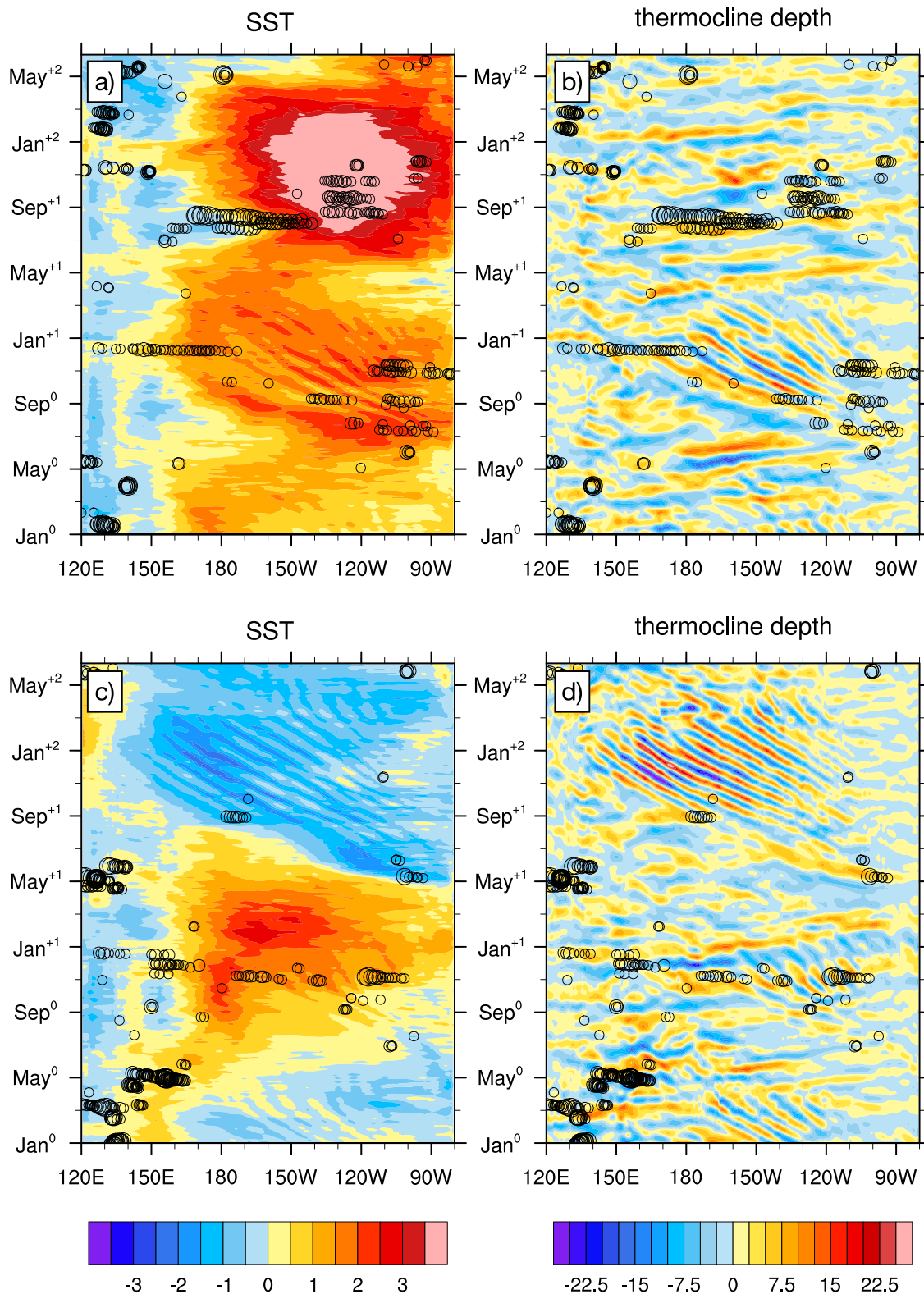


**Figure 3.** Case studies of El Niño events in LR-TC. Hovmöller diagrams of equatorial daily (a), (c) SST anomalies and (b), (d) thermocline depth anomalies in two El Niño events in the LR-TC. The anomalies are referenced to the long-term mean daily climatology. The thermocline depth anomalies are filtered with a band pass of 20–100 days. The black circles indicate the occurrences of the near-equatorial TC days. The event at the top is followed by another El Niño—the strongest extreme event in the LR-TC. Note that the early season TCs in the western Pacific excite eastward Kelvin waves.

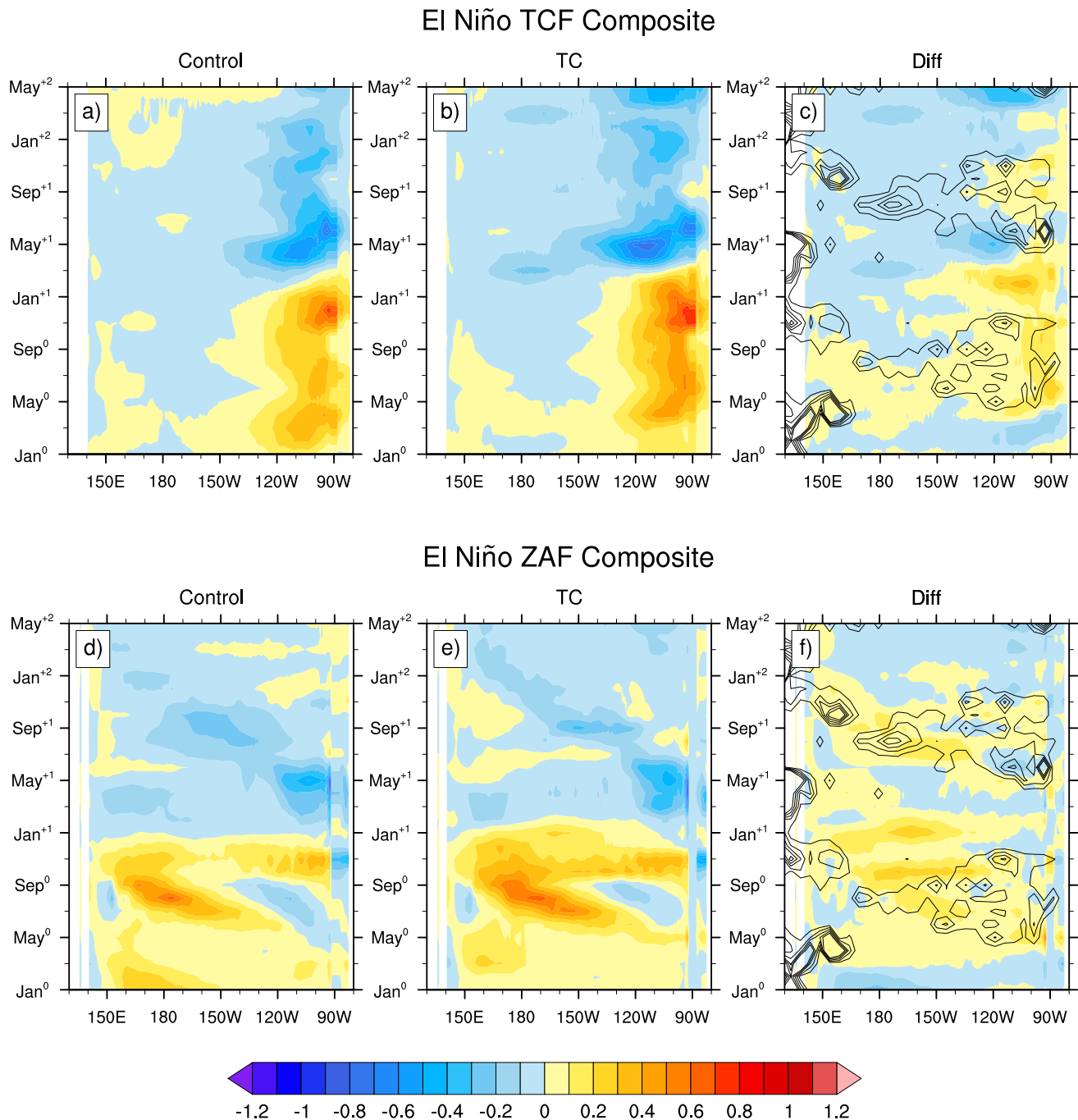


**Figure 4.** Composite Hovmöller diagrams of the (a)–(c) thermocline feedback term (TCF) and the (d)–(f) zonal advection feedback term (ZAF) in the SST tendency equation in the (a), (d) control simulation, (b), (e) TC simulation, and (c), (f) their differences (unit: °C/month). The black contours in the right most columns represent the integrated near-equatorial TC wind power (TC PDI, scaled by  $2.1 \times 10^{-8}$ ).

TC-induced thermocline deepening on El Niño growth. In addition, at the end of the El Niño life cycle when the equatorial thermocline shoals, TC-induced local thermocline deepening can reduce the associated SST cooling, affecting the transition to another ENSO state.

The zonal advection feedback in LR-TC is also increased (Figures 3d–3f). The model differences in the zonal advection feedback are comparable in magnitude to that in the thermocline feedback. The enhanced zonal advection feedback is attributed to the stronger eastward currents associated with the TCs in LR-TC (Figure 2i), and the increase of the feedback is mainly in the central equatorial Pacific during the El Niño developing phase.



#### 4. Conclusions

We investigate the climatological impact of TC winds on ENSO using a suite of simulations with a fully coupled Earth system model. The impact of TC winds is isolated by prescribing TC surface wind stress, extracted from a high-resolution TC permitting model, into a 1° model that has no intrinsic near-equatorial strong TCs. We show that the added TC winds can shift ENSO frequency, improve ENSO phase-locking, and enhance El Niño strength, bringing all in closer agreement with observations. TCs' influences on ENSO frequency and phase-locking are likely through their climatological impact on the background mean state, particularly the upper ocean thermal structure in the tropical Pacific. The dynamical processes and the dependence on TC characteristics need to be addressed in future studies. Additionally, we find that the integrated TC wind power correlates with the strong El Niño. TCs' impact on El Niño is manifested in the warmer eastern equatorial Pacific SST, eastward-propagating thermocline deepening, and enhanced eastward wind stress and surface current. We find that these TC-induced climatological changes are essential to El Niño dynamics through enhanced thermocline feedback and zonal advection feedback. This study verified in a fully coupled comprehensive Earth system model that the TCs are active participants in ENSO dynamics, as first hypothesized by Sobel and Camargo (2005) and Camargo and Sobel (2005).

An important aspect of TCs' climatological influence on El Niño is their synergetic annual cycle. The early season TCs in the near-equatorial western Pacific contribute to stronger WWBs, critical for El Niño development; eastern Pacific TC season during May–October brings increased near-equatorial TC winds, priming a deeper and warmer thermocline that enhances the thermocline feedback as El Niño approaches the peak; their effect continues in the following TC season as El Niño dissipates, affecting the transition to the next ENSO state. The influence of the synergetic annual cycle on ENSO dynamics is worth further investigations.

In the real world where ENSO has a strong modulation on TCs, our results suggest that a previously unidentified positive feedback mechanism likely exists between the climatological TCs and the observed ENSO characteristics. For example, during El Niño years, especially the stronger eastern Pacific El Niño type, enhanced TC activity often occurs in the near-equator central-to-eastern Pacific (i.e., Lin et al., 2020). Results in this study suggest that this may be a result of mutual enhancements—El Niño creates favorable conditions for TCs, and TCs provide fuel for El Niño through a series of ocean-atmosphere interactions. If TCs were not a part of the climate system, this feedback would be non-existent, and ENSO may not perform as we observe it today. However, since the TC surface winds are added directly at the air-sea interface in the model, the associated convective processes are not accounted for. An intriguing next step is to examine the impact of TC convection and precipitation on ENSO-related environmental factors and further investigate the feedback mechanisms. In addition, results from the current study are based on a single Earth system model. Investigation on model dependence is needed in future studies.

The model experiment in this study allows an isolation of the impact of TC winds on ENSO from their interwoven two-way interaction, which is difficult to achieve in observational studies. The experiment uses TCs winds extracted from the high-resolution TC-permitting model to mimic the model behavior where the impact of the models' self-generated TCs are implicitly included. Our findings about TCs' climatological role in shaping ENSO characteristic therefore have important implications for understanding not only the role TCs play in general in the climate system, but also the uncertainties of the simulated ENSO characteristics in the high-resolution models in current and future climate.

#### Data Availability Statement

The observation-based NOAA Extended Reconstructed Sea Surface Temperature (SST) V5 (ERSSTv5) reanalysis data is available at <https://www.ncei.noaa.gov/products/extended-reconstructed-sst>. The analysis code developed for this study is available at [https://github.com/huili77/TC\\_ENSO/](https://github.com/huili77/TC_ENSO/). Data products created for this study is made available open source on Zenodo (<https://doi.org/10.5281/zenodo.7236208>).

## Acknowledgments

Portions of this study were supported by the Regional and Global Model Analysis (RGMA) component of the Earth and Environmental System Modeling Program of the U.S. Department of Energy (DOE)'s Office of Biological & Environmental Research (BER) via National Science Foundation (NSF) IA 1947282, and under Award Number DE-SC0022070. This work also was supported by the National Center for Atmospheric Research, which is a major facility sponsored by the (NSF) under Cooperative Agreement No. 1852977. This research used resources of the Argonne Leadership Computing Facility, which is a DOE Office of Science User Facility supported under Contract DE-AC02-06CH11357. The research also used resources of the National Energy Research Scientific Computing Center (NERSC), a U.S. DOE Office of Science User Facility located at Lawrence Berkeley National Laboratory, operated under Contract No. DE-AC02-05CH11231. Additional computational and storage resources, including the Cheyenne Supercomputer (<https://doi.org/10.5065/D6RX99HX>), were provided by the Computational and Information Systems Laboratory (CISL) at NCAR. We thank Kerry Emanuel for providing the observed tropical cyclone tracks (<https://emanuel.mit.edu/products>).

## References

- An, S.-I., Kug, J.-S., Ham, Y.-G., & Kang, I.-S. (2008). Successive modulation of ENSO to the future greenhouse warming. *Journal of Climate*, 21(1), 3–21. <https://doi.org/10.1175/2007jcli1500.1>
- An, S.-I., & Wang, B. (2001). Mechanisms of locking of the El Niño and La Niña mature phases to boreal winter. *Journal of Climate*, 14(9), 2164–2176. [https://doi.org/10.1175/1520-0442\(2001\)014<2164:molote>2.0.co;2](https://doi.org/10.1175/1520-0442(2001)014<2164:molote>2.0.co;2)
- Bell, R., Hodges, K., Vidale, P. L., Strachan, J., & Roberts, M. (2014). Simulation of the global ENSO–tropical cyclone teleconnection by a high-resolution coupled general circulation model. *Journal of Climate*, 27(17), 6404–6422. <https://doi.org/10.1175/JCLI-D-13-00559.1>
- Camargo, S. J., Emanuel, K. A., & Sobel, A. H. (2007). Use of a genesis potential index to diagnose ENSO effects on tropical cyclone genesis. *Journal of Climate*, 20(19), 4819–4834. <https://doi.org/10.1175/JCLI4282.1>
- Camargo, S. J., & Sobel, A. H. (2005). Western North Pacific tropical cyclone intensity and ENSO. *Journal of Climate*, 18(15), 2996–3006. <https://doi.org/10.1175/jcli3457.1>
- Camargo, S. J., Sobel, A. H., Barnston, A. G., & Klotzbach, P. J. (2010). The influence of natural climate variability on tropical cyclones, and seasonal forecasts of tropical cyclone activity. In J. C. L. Chan & J. D. Kepert (Eds.), *Global perspectives on tropical cyclones* (pp. 325–360). World Scientific. [https://doi.org/10.1142/9789814293488\\_0011](https://doi.org/10.1142/9789814293488_0011)
- Chan, J. C. L. (2000). Tropical cyclone activity over the western North Pacific associated with El Niño and La Niña events. *Journal of Climate*, 13(16), 2960–2972. [https://doi.org/10.1175/15200442\(2000\)013<2960:TCAOTW.2.0.CO;2](https://doi.org/10.1175/15200442(2000)013<2960:TCAOTW.2.0.CO;2)
- Chand, S. S., McBride, J. L., Tory, K. J., Wheeler, M. C., & Walsh, K. J. E. (2013). Impact of different ENSO regimes on southwest Pacific tropical cyclones. *Journal of Climate*, 26(2), 600–608. <https://doi.org/10.1175/JCLI-D-12-00114.1>
- Chang, P., Zhang, S., Danabasoglu, G., Yeager, S. G., Fu, H., Wang, H., et al. (2020). An unprecedented set of high-resolution Earth system simulations for understanding multiscale interactions in climate variability and change. *Journal of Advances in Modeling Earth Systems*, 12(12), e2020MS002298. <https://doi.org/10.1029/2020ms002298>
- Clarke, A. J. (2008). *An introduction to the dynamics of El Niño & the southern oscillation*. Academic Press.
- Deng, L., Yang, X., & Xie, Q. (2010). ENSO frequency change in coupled climate models as response to the increasing CO<sub>2</sub> concentration. *Chinese Science Bulletin*, 55(8), 744–751. <https://doi.org/10.1007/s11434-009-0491-x>
- Emanuel, K. (2001). Contribution of tropical cyclones to meridional heat transport by the oceans. *Journal of Geophysical Research*, 106(D14), 14771–14781. <https://doi.org/10.1029/2000JD900641>
- Emanuel, K. (2005). Increasing destructiveness of tropical cyclones over the past 30 years. *Nature*, 436(7051), 686–688. <https://doi.org/10.1038/nature03906>
- Fedorov, A. V., Brierley, C. M., & Emanuel, K. (2010). Tropical cyclones and permanent El Niño in the early Pliocene epoch. *Nature*, 463(7284), 1066–1070. <https://doi.org/10.1038/nature08831>
- Fedorov, A. V., Hu, S., Lengaigne, M., & Guilyardi, E. (2015). The impact of westerly wind bursts and ocean initial state on the development, and diversity of El Niño events. *Climate Dynamics*, 44(5–6), 1381–1401. <https://doi.org/10.1007/s00382-014-2126-4>
- Fedorov, A. V., & Philander, S. G. (2000). Is El Niño changing? *Science*, 288(5473), 1997–2002. <https://doi.org/10.1126/Science.288.5473.1997>
- Fedorov, A. V., & Philander, S. G. (2001). A stability analysis of tropical ocean–atmosphere interactions: Bridging measurements and theory for El Niño. *Journal of Climate*, 14(14), 3086–3101. [https://doi.org/10.1175/1520-0442\(2001\)014<3086:Asaoto>2.0.CO;2](https://doi.org/10.1175/1520-0442(2001)014<3086:Asaoto>2.0.CO;2)
- Gebbie, G., Eisenman, I., Wittenberg, A., & Tziperman, E. (2007). Modulation of westerly wind bursts by sea surface temperature: A semistochastic feedback for ENSO. *Journal of the Atmospheric Sciences*, 64(9), 3281–3295. <https://doi.org/10.1175/jas4029.1>
- Ham, Y. G., & Kug, J. S. (2014). ENSO phase-locking to the boreal winter in CMIP3 and CMIP5 models. *Climate Dynamics*, 43(1–2), 305–318. <https://doi.org/10.1007/s00382-014-2064-1>
- Harrison, D. E., & Giese, B. S. (1991). Episodes of surface westerly winds as observed from islands in the western tropical Pacific. *Journal of Geophysical Research*, 96(Suppl), 3221–3237. <https://doi.org/10.1029/90JC01775>
- Harrison, D. E., & Vecchi, G. A. (1999). On the termination of El Niño. *Geophysical Research Letters*, 26(11), 1593–1596. <https://doi.org/10.1029/1999GL900316>
- Hartten, L. (1996). Synoptic settings of westerly wind bursts. *Journal of Geophysical Research*, 101(D12), 16997–17019. <https://doi.org/10.1029/96JD00030>
- Huang, B., Thorne, P. W., Banzon, V. F., Boyer, T., Chepurin, G., Lawrimore, J. H., et al. (2017). Extended reconstructed sea surface temperature version 5 (ERSSTv5), upgrades, validations, and intercomparisons. *Journal of Climate*, 30(4), 811–829. <https://doi.org/10.1175/JCLI-D-16-0836.1>
- Jin, F.-F. (1997). An equatorial ocean recharge paradigm for ENSO. Part I: Conceptual model. *Journal of the Atmospheric Sciences*, 54(7), 811–829. [https://doi.org/10.1175/1520-0469\(1997\)054<0811:AEORPF>2.0.CO;2](https://doi.org/10.1175/1520-0469(1997)054<0811:AEORPF>2.0.CO;2)
- Jin, F.-F., Kim, S. T., & Bejarano, L. (2006). A coupled-stability index for ENSO. *Geophysical Research Letters*, 33(23), L23708. <https://doi.org/10.1029/2006GL027221>
- Kang, I.-S., An, S.-I., & Jin, F.-F. (2001). A systematic approximation of the SST anomaly equation for ENSO. *Journal of the Meteorological Society of Japan. Ser. II*, 79, 1–10. <https://doi.org/10.2151/jmsj.79.1>
- Keen, R. A. (1982). The role of cross-equatorial tropical cyclone pairs in the southern oscillation. *Monthly Weather Review*, 110(10), 1405–1416. [https://doi.org/10.1175/1520-0493\(1982\)110<1405:TROCET>2.0.CO;2](https://doi.org/10.1175/1520-0493(1982)110<1405:TROCET>2.0.CO;2)
- Kessler, W. S. (2002). Is ENSO a cycle or a series of events? *Geophysical Research Letters*, 29(23), 401–404. <https://doi.org/10.1029/2002gl015924>
- Kug, J. S., Jin, F. F., & An, S. I. (2009). Two types of El Niño events: Cold tongue El Niño and warm pool El Niño. *Journal of Climate*, 22(6), 1499–1515. <https://doi.org/10.1175/2008jcli2624.1>
- Lander, M. A. (1994). An exploratory analysis of the relationship between tropical storm formation in the western North Pacific and ENSO. *Monthly Weather Review*, 122(4), 636–651. [https://doi.org/10.1175/1520-0493\(1994\)122<0636:aeaoir>2.0.co;2](https://doi.org/10.1175/1520-0493(1994)122<0636:aeaoir>2.0.co;2)
- Lengaigne, M., Guilyardi, E., Boulanger, J. P., Menkes, C., Delecluse, P., Inness, P., et al. (2004). Triggering of El Niño by westerly wind events in a coupled general circulation model. *Climate Dynamics*, 23(6), 601–620. <https://doi.org/10.1007/S00382-004-0457-2>
- Li, H., Hu, A., Meehl, G., Rosenbloom, N., & Strand, G. (2022). Impact of tropical cyclone wind forcing on the global climate in a fully-coupled climate model. *Journal of Climate*, 36(1), 111–129. <https://doi.org/10.1175/JCLI-D-22-0211.1>
- Li, H., & Srivier, R. L. (2016). Effects of ocean grid resolution on tropical cyclone-induced upper ocean responses using a global ocean general circulation model: Resolution affects ocean response to TC. *Journal of Geophysical Research: Oceans*, 121(11), 8305–8319. <https://doi.org/10.1002/2016JC011951>
- Li, H., & Srivier, R. L. (2018). Impact of tropical cyclones on the global ocean: Results from multi-decadal global ocean simulations isolating tropical cyclone forcing. *Journal of Climate*, 31(21), 8761–8784. <https://doi.org/10.1175/JCLI-D-18-0221.1>

- Lian, T., Chen, D., Tang, Y., Liu, X., Feng, J., & Zhou, L. (2018). Linkage between westerly wind bursts and tropical cyclones. *Geophysical Research Letters*, 45(20), 11431–11438. <https://doi.org/10.1029/2018GL079745>
- Lian, T., Ying, J., Ren, H.-L., Zhang, C., Liu, T., & Tan, X. X. (2019). Effects of tropical cyclones on ENSO. *Journal of Climate*, 32(19), 6423–6443. <https://doi.org/10.1175/jcli-d-18-0821.1>
- Liang, Y., & Fedorov, A. V. (2021). Linking the Madden–Julian Oscillation, tropical cyclones and westerly wind bursts as part of El Niño development. *Climate Dynamics*, 57(3–4), 1039–1060. <https://doi.org/10.1007/s00382-021-05757-1>
- Lin, I., Camargo, S. J., Patricola, C. M., Boucharel, J., Chand, S., Klotzbach, P., et al. (2020). El Niño Southern Oscillation in a changing climate. *Geophysical Monograph Series*, 377–408. <https://doi.org/10.1002/9781119548164.ch17>
- Lopez, H., Kirtman, B. P., Tziperman, E., & Gebbie, G. (2013). Impact of interactive westerly wind bursts on CCSM3. *Dynamics of Atmospheres and Oceans*, 59, 24–51. <https://doi.org/10.1016/j.dynatmoce.2012.11.001>
- Meehl, G. A., Yang, D., Arblaster, J. M., Bates, S., Rosenbloom, N., Neale, R., et al. (2019). Effects of model resolution, physics, and coupling on Southern Hemisphere storm tracks in CESM1.3. *Geophysical Research Letters*, 46(21), 12408–12416. <https://doi.org/10.1029/2019GL084057>
- Philander, S. G. (1990). *El Niño, La Niña, and the southern oscillation International geophysics series* (Vol. 46). Academic Press.
- Philander, S. G., & Fedorov, A. (2003). Is El Niño sporadic or cyclic? *Annual Review of Earth and Planetary Sciences*, 31(1), 579–594. <http://doi.org/10.1146/Annurev.Earth.31.100901.141255>
- Ren, H.-L., & Jin, F.-F. (2013). Recharge oscillator mechanisms in two types of ENSO. *Journal of Climate*, 26(17), 6506–6523. <https://doi.org/10.1175/JCLI-D-12-00601.1>
- Roundy, P. E., & Kiladis, G. N. (2006). Observed relationships between oceanic kelvin waves and atmospheric forcing. *Journal of Climate*, 19(20), 5253–5272. <https://doi.org/10.1175/JCLI3893.1>
- Sarachik, E. S., & Cane, M. A. (2010). *The El Niño–Southern oscillation phenomenon*. Cambridge University Press.
- Sobel, A. H., & Camargo, S. J. (2005). Influence of western North Pacific tropical cyclones on their environment. *Journal of the Atmospheric Sciences*, 62(9), 3396–3407. <https://doi.org/10.1175/JAS3539.1>
- Sobel, A. H., Camargo, S. J., Barnston, A. G., & Tippett, M. K. (2016). Northern hemisphere tropical cyclones during the quasi–El Niño of late 2014. *Natural Hazards*, 83(3), 1717–1729. <https://doi.org/10.1007/s11069-016-2389-7>
- Thompson, C. J., & Battisti, D. S. (2001). A linear stochastic dynamical model of ENSO. Part II: Analysis. *Journal of Climate*, 14(4), 445–466. [https://doi.org/10.1175/1520-0442\(2001\)014<0445:Alsdm0>2.0.Co;2](https://doi.org/10.1175/1520-0442(2001)014<0445:Alsdm0>2.0.Co;2)
- Tziperman, E., Cane, M. A., & Blumenthal, B. (1998). Locking of El Niño peak time to the end of the calendar year in the delayed oscillator picture of ENSO. *Journal of Climate*, 11, 2191–2203.
- Tziperman, E., Zebiak, S. E., & Cane, M. A. (1997). Mechanisms of seasonal–ENSO interaction. *Journal of the Atmospheric Sciences*, 54(1), 61–71. [https://doi.org/10.1175/1520-0469\(1997\)054<0061:MOSEI%3E2.0.CO;2](https://doi.org/10.1175/1520-0469(1997)054<0061:MOSEI%3E2.0.CO;2)
- Ullrich, P. A., & Zarzycki, C. M. (2017). TempestExtremes: A framework for scale-insensitive pointwise feature tracking on unstructured grids. *Geoscientific Model Development*, 10(3), 1069–1090. <https://doi.org/10.5194/gmd-10-1069-2017>
- Ullrich, P. A., Zarzycki, C. M., McClenney, E. E., Pinheiro, M. C., Stansfield, A. M., & Reed, K. A. (2021). TempestExtremes v2.1: A community framework for feature detection, tracking, and analysis in large datasets. *Geoscientific Model Development*, 14(8), 5023–5048. <https://doi.org/10.5194/gmd-14-5023-2021>
- Wang, B., & Chan, J. C. L. (2002). How strong ENSO events affect tropical storm activity over the western North Pacific. *Journal of Climate*, 15(13), 1643–1658. [https://doi.org/10.1175/15200442\(2002\)015<1643:HSEEAT>2.0.CO;2](https://doi.org/10.1175/15200442(2002)015<1643:HSEEAT>2.0.CO;2)
- Wang, Q., & Li, J. (2022). Feedback of tropical cyclones on El Niño diversity. Part II: Possible mechanism and prediction. *Climate Dynamics*, 59(3–4), 715–735. <https://doi.org/10.1007/s00382-022-06150-2>
- Wang, Q. Y., Li, J. P., Jin, F.-F., Chan, J. C. L., Wang, C. Z., Ding, R. Q., et al. (2019). Tropical cyclones act to intensify El Niño. *Nature Communications*, 10(1), 3793. <https://doi.org/10.1038/s41467-019-11720-w>